

Kinetic Study of Boric Acid–Borate Interchange in Aqueous Solution by ^{11}B NMR SpectroscopyKoji Ishihara,^{a,1a} Akira Nagasawa,^{1b} Kimiko Umemoto,^{1c} Hideaki Ito,^{1a} and Kazuo Saito^{1c}

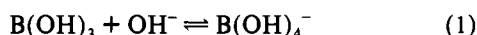
Department of Chemistry, School of Science and Engineering, Waseda University, Okubo, Shinjuku, Tokyo 169, Japan, Department of Chemistry, Faculty of Science, Saitama University, Urawa 338, Japan, and Division of Natural Science, International Christian University, Mitaka, Tokyo 181, Japan

Received December 14, 1993^o

Kinetics of interchange between boric acid and tetrahydroxyborate has been studied by the band shape analysis of ^{11}B NMR signals in aqueous solution of pH 8–10 at 20–52 °C and 0.1–250 MPa. The system was analyzed as two-site exchange $\text{B}(\text{OH})_3 \rightleftharpoons \text{B}(\text{OH})_4^-$. The observed first-order rate constant toward the right (k_X) is related to the second-order exchange rate constant (k_{ex}) by the equation $k_X = k_{\text{ex}} C_T [\text{OH}^-] / (k_b + [\text{OH}^-])$, where $k_b = [\text{B}(\text{OH})_3][\text{OH}^-] / [\text{B}(\text{OH})_4^-]$, and C_T is the total concentration of boron. Under the given conditions k_{ex} is $(2-7) \times 10^6 \text{ dm}^3 \text{ mol}^{-1} \text{ s}^{-1}$ and ΔH^\ddagger , ΔS^\ddagger , and ΔV^\ddagger are $20.1 \pm 1.0 \text{ kJ mol}^{-1}$, $-55.0 \pm 3.1 \text{ J mol}^{-1} \text{ K}^{-1}$, and $-9.9 \pm 0.5 \text{ cm}^3 \text{ mol}^{-1}$, respectively. The activation parameters reflect the transition state forming dimeric $[(\text{OH})_3\text{B}(\mu\text{-OH})\text{B}(\text{OH})_3]^-$. The results are compared with those of related reactions.

Introduction

Whereas most oxoanions of non-metallic elements undergo protonation and deprotonation without involving substantial structural change, boron is a unique element in which planar oxoacid $\text{B}(\text{OH})_3$ is converted into tetrahedral oxoanion $\text{B}(\text{OH})_4^-$ in a basic solution. The equilibrium of eq 1 has been extensively



$$K_a = [\text{B}(\text{OH})_4^-] K_w / [\text{B}(\text{OH})_3][\text{OH}^-]; K_w = [\text{H}^+][\text{OH}^-]$$

studied by Ingri ($\text{p}K_a = 8.98$ at 25 °C, ionic strength $I = 0.1 \text{ M}$, $M = \text{mol dm}^{-3}$).²

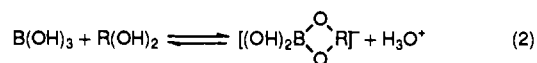
Boric acid tends to give polymerized anions such as $\text{B}_3\text{O}_3(\text{OH})_4^-$.³ The monomeric form is exclusively present only in $<0.025 \text{ M}$ aqueous solution. The polymerization equilibrium of boric acid was studied by ^{11}B NMR spectroscopy by Salentine,⁴ Momii and Nachtrieb,⁵ and Smith and Wiersema,⁶ but no discussion was made as to the dynamic behavior.

As for the dynamics, Gilkerson⁷ observed dielectric dispersion of boric acid in 1957 and discussed the rate of combination between H^+ and H_2BO_3^- , but the structure of borate ion was not well identified. Yasunaga et al.⁸ measured the ultrasonic absorption of 0.05 to 0.2 M “metaborate” solution and discussed the relaxation accompanied by the “hydrolysis”, but the ionic form was not well characterized.

Anderson et al.⁹ predicted in their kinetic studies of polyborate formation by the temperature jump method that the second-order rate constant of the forward reaction of eq 1 would be $\approx 10^{10} \text{ M}^{-1} \text{ s}^{-1}$. Waton et al. studied the relaxation of 0.1–10 mM boric acid solutions with thymol blue as indicator by the

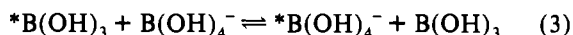
temperature jump method.¹⁰ They obtained the second order rate constant of the forward reaction of eq 1 ($10.7 \times 10^6 \text{ M}^{-1} \text{ s}^{-1}$ at 25 °C), and calculated ΔH^\ddagger and ΔS^\ddagger to be 14.6 kJ mol⁻¹ and -60.6 J mol⁻¹ K⁻¹, respectively.

Boric acid forms chelate rings with 1,2-dihydric alcohols and related organic compounds, and the equilibrium was studied by ^1H , ^{11}B , and ^{13}C NMR measurement.¹¹ One of the present authors studied the kinetics of chelate formation between boric acid and 4-isopropyltropolone, chromotropic acid, and a tridentate H-resorcinol in solution by the stopped-flow spectrophotometry at pH ≈ 4 .¹² Equation 2 also involves structure change from planar



triangle to tetrahedral around B atom. We have planned to clarify the dynamics of such change with reference to eq 1.

Since NMR spectroscopy provides structural information around the boron atom, we planned to use the ^{11}B signal for elucidating the kinetics of structural change accompanied by eq 1. The change of chemical shift and line width of ^{11}B signals of monomeric boric acid was studied by Balz et al. by use of solutions of $\text{B}_4\text{O}_7^{2-}$, B_5O_8^- , and metaborate BO_2^- at pH 2–12.5, but no kinetic discussion was made.¹³ We observed only one coalesced signal in slightly basic aqueous solution. We have measured the NMR signals in 0.007–0.017 M boric acid solutions of pH 8–10 at 5–52 °C and 0.1–250 MPa. The results were analyzed to find that the following two-site interchange (eq 3) is responsible for



the change in NMR signals under the given conditions. This paper gives detailed results of the kinetic studies and discusses the mechanism of this reaction.

- * To whom correspondence should be addressed.
^o Abstract published in *Advance ACS Abstracts*, July 15, 1994.
 (1) (a) Waseda University. (b) Saitama University. (c) International Christian University.
 (2) Ingri, N. *Acta Chem. Scand.* **1962**, *16*, 439.
 (3) (a) Antikainen, P. J. *Suom. Kemistil.* **1957**, *B30*, 74. (b) Lourijssen-Teyssèdre, M. *Bull. Soc. Chim. Fr.* **1955**, 1111.
 (4) Salentine, C. G. *Inorg. Chem.* **1983**, *22*, 3920.
 (5) Momii, R. K.; Nachtrieb, N. H. *Inorg. Chem.* **1967**, *6*, 1189.
 (6) Smith, H. D., Jr.; Wiersema, R. J. *Inorg. Chem.* **1972**, *11*, 1152.
 (7) Gilkerson, W. R. *J. Chem. Phys.* **1957**, *27*, 914.
 (8) Yasunaga, T.; Tatsumoto, N.; Miura, M. *J. Chem. Phys.* **1965**, *43*, 2745.
 (9) Anderson, J. L.; Eyring, E. M.; Whittaker, M. P. *J. Phys. Chem.* **1964**, *68*, 1128.

- (10) Waton, G.; Mallo, P.; Candau, S. J. *J. Phys. Chem.* **1984**, *88*, 3301.
 (11) (a) Henderson, W. G.; How, M. J.; Kennedy, G. R.; Mooney, E. F. *Carbohydr. Res.* **1973**, *28*, 1. (b) van Duin, M.; Peters, J. A.; Kieboom, A. P. G.; van Bekkum, H. *J. Chem. Soc., Dalton Trans.* **1987**, 2051 and references therein. (c) Coddington, J. M.; Taylor, M. J. *J. Coord. Chem.* **1989**, *20*, 27.
 (12) Ishihara, K.; Mouri, Y.; Funahashi, S.; Tanaka, M. *Inorg. Chem.* **1991**, *30*, 2356.
 (13) Balz, R.; Brandle, U.; Kammerer, E.; Kohnlein, D.; Lutz, O.; Nolle, A.; Schafitel, R.; Veil, E. *Z. Naturforsch.* **1986**, *41A*, 737.

Experimental Section

Reagents. Reagent grade boric acid (Wako Pure Chemical Industries, Osaka) was recrystallized from hot water and dried in vacuo. Carbonate-free NaOH solution was prepared by the usual method. The ionic strength was adjusted with NaClO₄ solutions prepared from the recrystallized salt.¹⁴ All the solutions for NMR measurements were prepared with doubly distilled water containing 20% D₂O, and high purity nitrogen was bubbled for at least 10 min.

Measurements. The NMR measurements under atmospheric pressure were performed in standard Pyrex sample tubes of 5 mm diameter with a Varian XL-300 FT-NMR spectrometer operated at 96.25 MHz between 5 and 52 °C. The pulse width was 15.0 μs (45° pulse), the pulse repetition time was 1.4 s, and the number of scans was 2048. NMR measurements under elevated pressure (up to 250 MPa) were made by a JEOL JNM-EX270WB FT-NMR spectrometer at 86.67 MHz with a high-pressure probe¹⁵ at 20 and 33 °C (without spinning). The pulse width, and pulse repetition time were 9.9 μs (90° pulse) and 1 s (acquisition time 0.256 s), respectively, and 40 960 (20 °C) and 76 800 (33 °C) scans were accumulated. The hydrogen ion concentration was measured at 25 °C with a pH meter (Model E654, Metrohm; glass electrode combined with saturated calomel electrode containing NaCl) on the potentiometric scale, by use of solutions containing the same concentrations of boron, NaOH, and NaClO₄ (but without D₂O) as those used for the NMR measurement. The theoretical relationship between the hydrogen ion concentration and the potential was employed, and a 1.00 × 10⁻² M HClO₄ solution of ionic strength 0.10 M (NaClO₄) was used as the standard. The hydrogen ion exponent in 20% D₂O was estimated by assuming the additivity law between pK_w values (ion product exponent) of H₂O and D₂O at varying temperatures. Necessary data were obtained in the literature.¹⁶ All the estimated values are shown in the supplementary material.

The temperature was measured with a thermocouple placed just outside of the sample tube in the probe. The observed temperature was calibrated by use of an empirical formula, which shows the relationship between the real temperature and the separation of chemical shifts between δ(CH₃) and δ(OH) of methanol placed at the position of the sample solution in the probe.^{17,18} The temperature coefficient of the chemical shift was measured by use of a sample tube with double walls containing sample solutions of pH 3 and 0.1 M NaOH. The pressure was measured with a pressure sensor (HT-3500, Orientec Corp., Tokyo) calibrated with a Heize Bourdon gauge.

Results

Band Shape Analysis. A sharp signal of the sample solution was superimposed by a very broad signal, which originates from the glass of the sample tube and in the probe. Observation of the difference spectrum clearly indicated that the half-width of the signals of interest was not affected by the broad signal.

The ¹¹B signals of the solutions are shown in Figure 1. The chemical shift δ(¹¹B) was referred to 0.012 M B(OH)₃ in an aqueous solution of pH = 3.0 (HClO₄) containing 20% D₂O; δ(¹¹B) of 0.012 M B(OH)₄⁻ in 0.1 M NaOH containing 20% D₂O is -17.71 (25.8 °C), -17.65 (35.8 °C), -17.53 (43.6 °C), and -17.40 (51.8 °C), respectively, and is independent of the ionic strength (0.1–0.5 M). The observed pH dependence of chemical shift and bandwidth is very similar to the results of Balz et al.¹³ They pointed out an anomalous broadening in the pH region 8–10. We analyze the NMR pattern in this particular region in the following.

Only monomeric species exist in solutions of total boron concentration less than 0.025 M.¹⁹ Since the pK_a of boric acid is 8.98 (25 °C, I = 0.1 M), B(OH)₃ and B(OH)₄⁻ are present virtually exclusively in solutions of pH < 7 and > 11, respectively.

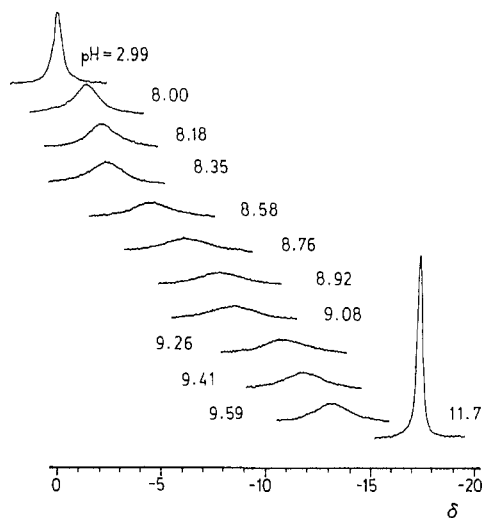


Figure 1. ¹¹B chemical shift as a function of pH. C_T = 0.0120 M; I = 0.10 M; T = 35.8 °C.

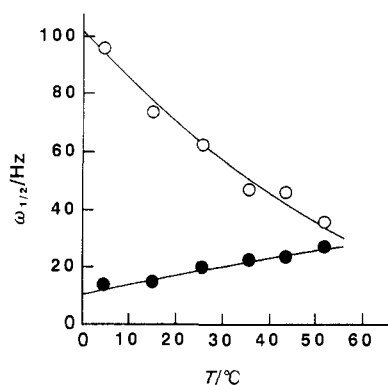


Figure 2. Change of bandwidth $\omega_{1/2}$ with temperature: Open circle at pH 3.0; filled circle at pH 13.

Both species coexist in self-buffered solutions of pH 8–10, but a single broad peak was observed at each pH in this region. Dependence of chemical shift on pH gave a pK_a of 9.20 (at 25.8 °C, I = 0.10 M (20% D₂O, NaClO₄)) for the system.

There should be a rapid chemical exchange between B(OH)₃ (site X) and B(OH)₄⁻ (site Y). For analyzing the NMR patterns in Figure 1 in terms of a two-site exchange (eq 4), “intrinsic”



bandwidths of both species should be known under the given experimental conditions at each temperature and pressure. We consider that the bandwidths at pH 3 (Figure 1) and in 0.1 M NaOH solution (not shown in Figure 1) represent the “intrinsic” values of B(OH)₃ and B(OH)₄⁻, respectively, by the following reasons.

The change in band width $\omega_{1/2}$ with temperature at pH 3.0 and in 0.1 M NaOH solution (pH ≈ 13) is shown in Figure 2, and the NMR signals at pH 1.0, 8.8, and 13.0 under elevated pressures are given in Figure 3.

The bandwidth of NMR signals is governed by various factors, but one of the most important factors in the present system should be the site exchange involving individual species. Under such conditions as pH 1–7 and pH 11–13, B(OH)₃ and B(OH)₄⁻ overwhelm other species in solution, respectively, and no appreciable change in chemical shift would be expected even if site exchange is taking place. If the $\omega_{1/2}$ values in Figure 2 reflected the exchange of eq 1, the relationship between $\omega_{1/2}$ and absolute temperature should be similar to each other at pH 3 and 13, but the trend is reversed. Hence the temperature dependence of the

(14) Funahashi, S.; Haraguchi, K.; Tanaka, M. *Inorg. Chem.* **1977**, *16*, 1349.

(15) Ishii, M.; Funahashi, S.; Ishihara, K.; Tanaka, M. *Bull. Chem. Soc. Jpn.* **1989**, *62*, 1852.

(16) (a) Bates, R. G. *Determination of pH*; Wiley: New York, 1964; pp 112–221. (b) Covington, A. K.; Robinson, R. A.; Bates, R. G. *J. Phys. Chem.* **1966**, *70*, 3820.

(17) (a) Van Geet, A. L. *Anal. Chem.* **1968**, *40*, 2227. (b) Van Geet, A. L. *Anal. Chem.* **1970**, *42*, 679.

(18) Raiford, D. S.; Fisk, C. L.; Backer, E. D. *Anal. Chem.* **1979**, *51*, 2060.

(19) Cotton, F. A.; Wilkinson, G. *Advanced Inorganic Chemistry*, 5th ed.; Wiley-Interscience: New York, 1988; p 169.

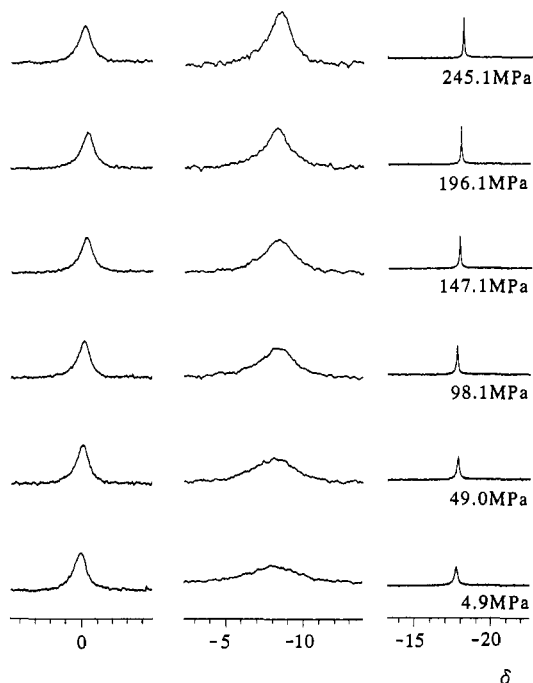


Figure 3. Pressure dependence of ^{11}B NMR signals. $C_T = 0.0120\text{ M}$; $I = 0.10\text{ M}$; $T = 20.0\text{ }^\circ\text{C}$; accumulation = 40960. pH under ambient pressure: left, 1.0; center, 8.8; right, 13.0.

$\omega_{1/2}$ values at pH 3 and 13 should be discussed individually. The change in $\omega_{1/2}$ at pH 8.8 must reflect the site exchange as shown below.

At pH 3 the bandwidth decreases with rise of temperature. Since ^{11}B nucleus with nuclear spin $3/2$ has nuclear quadrupole moment $e \times 0.0355 \times 10^{-24}\text{ cm}^2$ (e , charge of proton), and $\text{B}(\text{OH})_3$ has a rather low symmetry, D_{3h} , the quadrupolar relaxation may contribute to the bandwidth. The bandwidth $\omega_{1/2}$ is proportional to the correlation time τ_c which is equal to $\eta\nu/kT$, where η , ν , k , and T stand for the viscosity, the volume of solute molecule, the Boltzmann constant, and the absolute temperature, respectively. With rise of temperature the numerator decreases, and the denominator increases to decrease $\omega_{1/2}$.²⁰

If there were a rapid exchange between $\text{B}(\text{OH})_3$ and one or more hidden species, the observed signals would correspond to the coalesced peaks between them, and the sharp signals at elevated temperatures can be approximated as the "intrinsic" bandwidth of $\text{B}(\text{OH})_3$. However, when the bandwidth at a high temperature (30 Hz) was used in place of the value at 25 $^\circ\text{C}$ (60 Hz), the calculated k_X decreased only very slightly (from 1.38×10^4 to $1.30 \times 10^4\text{ s}^{-1}$). Hence, despite of the change in bandwidth with temperature, the observed bandwidth at a given temperature can be reckoned to represent the "intrinsic" bandwidths for $\text{B}(\text{OH})_3$ at the given temperature.

At pH 13 the signal is broadened with increase in temperature. Balz et al. measured the bandwidth of sodium metaborate (NaBO_2) and tetraborate ($\text{Na}_2\text{B}_4\text{O}_7$) and ammonium pentaborate ($\text{NH}_4\text{B}_5\text{O}_{13}$) as a function of the concentration.¹³ Although the composition of these polyborate species in solution was not well determined, the change in chemical shift of their solutions may reflect the change in composition of the borate in the given concentrations. Some other species than $\text{B}(\text{OH})_4^-$ can be present in the solutions, and the change in bandwidths of more than 0.03 M polyborate solutions would be caused by the exchange between $\text{B}(\text{OH})_4^-$ and one or more unknown species. Under our experimental conditions $\text{B}(\text{OH})_4^-$ should overwhelm other species and no change in chemical shift was observed. The broadening of the bands with rise of temperature at pH 13 (Figure 2) does

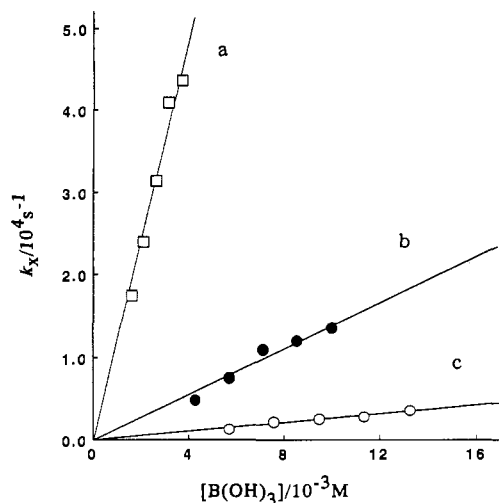


Figure 4. Dependence of k_X on the boric acid concentration. $I = 0.10\text{ M}$; $T = 35.8\text{ }^\circ\text{C}$; $[\text{OH}^-]/\text{M} = 4.07 \times 10^{-5}$ (a), 7.86×10^{-6} (b), 3.06×10^{-6} (c).

not seem to owe to nuclear quadrupole relaxation, because $\text{B}(\text{OH})_4^-$ is highly symmetrical. There is a possibility that the exchange between $\text{B}(\text{OH})_4^-$ and small amounts of hidden species is not very fast and the rate increases with rise of temperature to enhance the broadening.

The $\omega_{1/2}$ values at pH 1.0 does not change appreciably whereas that at pH 13 decreases with rise of pressure. Site exchange cannot be the reason of the decrease in bandwidth, but the real reason is unknown. For calculating the k_X value at a given pressure, the $\omega_{1/2}$ values at pH 1 and 13 at the given pressure were used as "intrinsic" bandwidths of $\text{B}(\text{OH})_3$ and $\text{B}(\text{OH})_4^-$, respectively. When the $\omega_{1/2}$ value at ambient pressure was used in calculating the k_X value at elevated pressures the difference was ca. 10%.

The band shape (Table SI) was analyzed by applying nonlinear least-squares fitting to Rogers and Woodbrey's equation,²¹ and the most suitable values of k_X and P_X were determined (Tables SII–SIV, supplementary material). P_X is the fractional population of ^{11}B in state X, and is related to that in state Y (P_Y) and to the rate constant by eqs 5 and 6, respectively. Multiplication of both

$$P_X + P_Y = 1 \quad (5)$$

$$k_X P_X = k_Y P_Y \quad (6)$$

sides of eq 6 by the total concentration of boron (C_T) gives eq 7.

$$k_X[\text{B}(\text{OH})_3] = k_Y[\text{B}(\text{OH})_4^-] \quad (7)$$

Influence of C_T and $[\text{OH}^-]$ on k_X . The k_X value increases with increase in C_T at a given hydroxide ion concentration. Figure 4 shows the linear relationship between k_X and $[\text{B}(\text{OH})_3]$ at the given concentration of hydroxide ion (cf. $(1 + K_b^{-1}[\text{OH}^-])^{-1}[\text{B}(\text{OH})_3] = C_T$ and $K_b = K_w/K_a$, eq 8). The plot of k_1 , the

$$k_X = k_1[\text{B}(\text{OH})_3] \quad (8)$$

gradient of Figure 4, against $[\text{OH}^-]$ (Figure 5) is linear with zero intercept, and its gradient k_2 is equal to $k_1/[\text{OH}^-]$. Thus eq 9

$$k_X = k_2[\text{OH}^-][\text{B}(\text{OH})_3] \quad (9)$$

is obtained. By considering the relationships of eqs 1 and 7, eqs 10 and 11 are derived from eq 9. Equation 11 means

(20) Abragam, A. *The Principles of Nuclear Magnetism*; Oxford University Press: Oxford, England, 1961; p 313.

(21) Rogers, M. T.; Woodbrey, J. C. *J. Phys. Chem.* **1962**, *66*, 540.

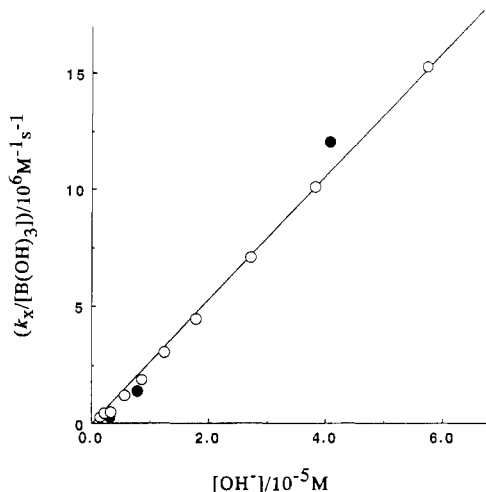


Figure 5. Dependence of $k_X/[B(OH)_3]$ on the hydrogen ion concentration. $I = 0.10$ M; $T = 35.8$ °C. Full circles represent the data obtained from the slope of straight lines of Figure 4.

$$k_X = k_2 K_b [B(OH)_4^-] = k_{ex} [B(OH)_4^-] \quad (10)$$

$$k_X [B(OH)_3] = k_{ex} [B(OH)_4^-] [B(OH)_3] \quad (11)$$

that the observed forward rate constant of eq 4 is equal to the intermolecular OH^- exchange rate constant k_{ex} (in $M^{-1} s^{-1}$) between boric acid and borate ion of eq 3 ($k_{ex} = k_2 K_b$).

Figure 6 shows that, at a given C_T , k_X increases with increase in $[OH^-]$ and then levels off. Obviously eq 9 is transformed to eq 12. At lower $[OH^-]$ ($K_b \ll [OH^-]$), k_X linearly increases with

$$k_X = k_{ex} C_T [OH^-] / (K_b + [OH^-]) \quad (12)$$

increase in $[OH^-]$ and approaches a constant value $k_{ex} C_T$ at a high $[OH^-]$ ($K_b \ll [OH^-]$). Optimum values of k_{ex} and K_b were calculated by applying nonlinear least-squares fitting to eq 12 and are shown in Table 1.

Influence of Temperature and Pressure. The activation enthalpy and entropy were calculated from the kinetic data at 25.8–51.8 °C. The volume of activation was calculated from the k_{ex} data at 20 and 33 °C and added to Table 1 with those of related reactions.

The temperature coefficients of the pK_a value of boric acid and of the ion product of H_2O and D_2O , and the deuterium effect on pK_a of boric acid were taken from ref 16 (the pK_a value calculated on the basis of chemical shift and half-value width of Figure 1 coincided with the literature value).

The activation volume was calculated as follows. Equation 10 is rewritten as eq 13. Although $[B(OH)_4^-]$ and C_T (in $mol\ dm^{-3}$)

$$k_{ex} = k_X / [B(OH)_4^-] = k_X / (C_T P_Y) \quad (13)$$

are dependent on the pressure, we can calculate the volume of activation for eq 3 from the pressure dependence of uncorrected k_{ex} (in $M^{-1} s^{-1}$) which is determined with molarity not at elevated pressure but at ambient pressure, as stated in the literature.^{22,23} Consequently, the second-order exchange rate constant at elevated pressure k_{ex}^p can be calculated from eq 14, where k_X^p and P_Y^p

$$k_{ex}^p = k_X^p / (C_T^1 P_Y^p) \quad (14)$$

are those obtained by band shape analysis at pressure p , and C_T^1 is the total molar concentration of boron at ambient pressure.

(22) Hamann, S. D.; le Noble, W. J. *J. Chem. Educ.* **1984**, *61*, 658.

(23) van Eldik, R., Ed.; *Inorganic High Pressure Chemistry: Kinetics and Mechanisms*; Elsevier: Amsterdam, 1986.

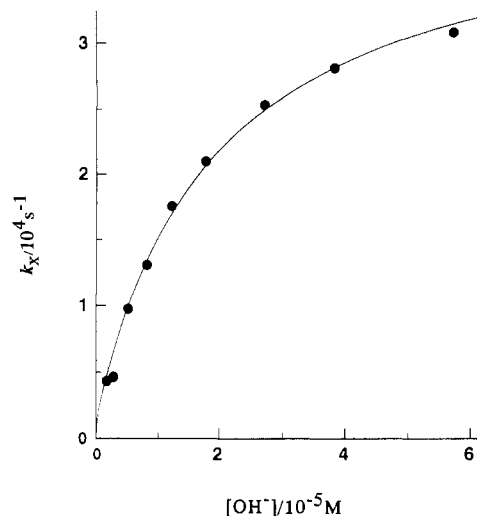


Figure 6. Dependence of k_X on hydrogen ion concentration. $C_T = 0.0120$ M; $I = 0.10$ M; $T = 35.8$ °C.

Table 1. Kinetic Parameters for the Borate–Boric Acid Exchange in Aqueous Solution

$k_{ex}/M^{-1} s^{-1}$ ($T/^\circ C$)	$\Delta H^\ddagger/kJ\ mol^{-1}$	$\Delta S^\ddagger/J\ mol^{-1} K^{-1}$	$\Delta V^\ddagger/cm^3\ mol^{-1}$
Boron Exchange ^a			
2.58×10^6 (25.8)			-10.3 ± 0.5^b
3.48×10^6 (35.8)	20.1 ± 1.0	-55.0 ± 3.1	-9.6 ± 0.7^c
4.45×10^6 (43.6)			
5.29×10^6 (51.8)			
[chelate formation] ^d			
Hipt 144 (25.0)	26.2 ± 0.7	-116 ± 4	-9.9 ± 0.3
H ₂ cht ²⁻ 1380 (25.0)	12.9 ± 1.5	-141 ± 5	-15.5 ± 1.9

^a At pH 8–10; $I = 0.1$ M. ^b At pH 8.8 and 20.0 °C. ^c At pH 9.3 and 33.1 °C. ^d k_f values; Hipt, 4-isopropyltropolone (hinokitiol); H₂cht, 1,8-dihydroxynaphthalene-3,6-disulfonic acid (chromotropic acid).¹²

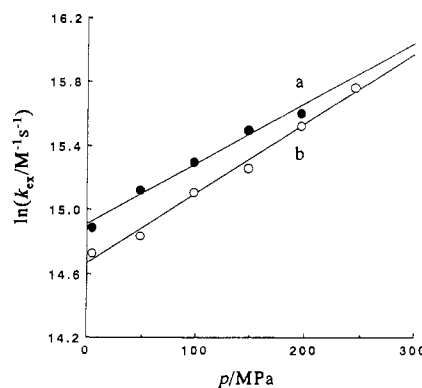
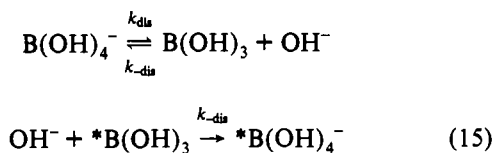


Figure 7. Dependence of the exchange rate constant k_{ex} upon pressure. $I = 0.10$ M. Key: a (full circle), at 33 °C; b (open circle), at 20 °C.

The k_{ex} value is shown in Table SIV and plotted against the pressure in Figure 7. The ΔV_{ex}^\ddagger values are shown in Table 1 together with other kinetic data.

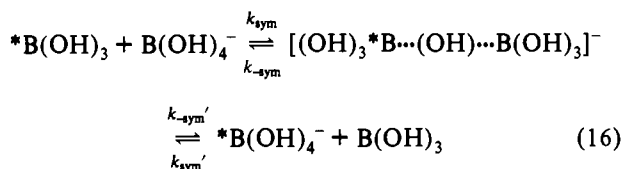
Discussion

Reaction Mechanism. The experimental results are appropriately analyzed as to reflect a two-site exchange shown by eq 3. Waton et al. obtained a second-order rate constant for the forward reaction of eq 1 (k_{-dis} , eq 15) of $10.7 \times 10^6\ M^{-1} s^{-1}$ at 25 °C.¹⁰ At pH ≈ 9 , the apparent first-order rate constant with respect to boric acid is calculated to be $\approx 10^2\ s^{-1}$. If the exchange between $B(OH)_3$ and $B(OH)_4^-$ proceeded through direct reaction (eq 15) at this rate, the NMR signals of both species should



appear as two individual peaks under the present experimental conditions. The fact that we observed a coalesced peak indicates that there should be another route which enables the exchange at the observed rate. We consider that the new route proceeds through a dimeric form on the following reasons: eq 11 indicates that the first-order rate constant k_X with respect to the concentration of B(OH)_3 is proportional to the concentration of B(OH)_4^- , the counterpart of the exchange reaction. Hence k_{ex} is a second-order rate constant, and a bimolecular mechanism is suggested for the exchange.

Equation 3 indicates a two-site exchange in an equilibrated state, and there is no net change in the concentrations of B(OH)_3 and B(OH)_4^- during the NMR measurement. Hence the reaction coordinate should satisfy a symmetrical energy profile. Generally, a dimer of oxoanions with a symmetric oxygen bridge between two identical non-metallic atoms is reckoned more stable than that with an asymmetrical bridge. Thus the symmetrical dimer should situate at the saddle point of the diagram as a reaction intermediate. Equation 16 indicates the most plausible reaction



mechanism. When a stationary state is assumed for the dimer, the exchange rate constant k_{ex} is expressed by eq 17. Since the

$$k_{ex} = k_{sym} k_{-sym}' / (k_{-sym} + k_{-sym}') \quad (17)$$

reaction coordinate is symmetrical, $k_{-sym} = k_{-sym}'$ and hence $k_{ex} = (1/2)k_{sym}$. Then the ΔS^\ddagger value for k_{sym} is smaller than the value in Table 1 by ca. $6 \text{ J mol}^{-1} \text{ K}^{-1}$. The step with k_{sym} (and k_{-sym}) is understood to be rate determining, and the observed ΔS^\ddagger and ΔV^\ddagger values reflect the ease of formation of the symmetrical dimer through the transition state.

Under the present experimental condition ($C_T < 0.025 \text{ M}$) monomeric B(OH)_3 and B(OH)_4^- are the overwhelmingly present species, and k_{ex} , which we have obtained from the rate equation, is a second-order rate constant. There is a possibility that a very small amount of trimeric species $\text{B}_3\text{O}_3(\text{OH})_4^-$ is present at the equilibrated state.^{4-6,11} However, a rate-determining termolecular reaction $2\text{B(OH)}_3 + \text{B(OH)}_4^- \rightarrow \text{B}_3\text{O}_3(\text{OH})_4^- + 3\text{H}_2\text{O}$ is unlikely. Kinetic data including activation parameters give information as to the transition state. The transition state we have postulated may reflect the first step of the oligomerization, and the site exchange of boron atoms must take place at this stage.

The activation parameters, particularly the volume of activation, support such a view. Generally an observed volume of activation reflects the change in the volume of reacting species and that in the solvation sphere (sheath effect) accompanied by the reaction. The latter effect is mostly governed by the change in ionic charge accompanied by the reaction.

We observed significantly negative volume of activation, and consider that the ΔV_{ex}^\ddagger value (ca. $-10 \text{ cm}^3 \text{ mol}^{-1}$) reflects the decrease in volume on going from the initial state to the transition state, which very likely has an asymmetrical $\text{B} \cdots (\text{OH}) \cdots \text{B}$ bridge. Such a dimer formation involves the change of two spheres

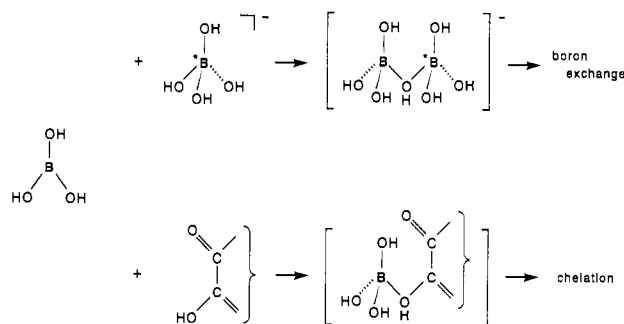


Figure 8. Schematic comparison of the association of B(OH)_3 with B(OH)_4^- and with a 1,2-dihydric alcohol.

(B(OH)_4^- and B(OH)_3)²⁴ into a spheroidal, and results in a significant decrease in volume. The change in solvation accompanied by the conversion of B(OH)_3 without charge and the univalent anion B(OH)_4^- into a large univalent anion $[(\text{HO})_3\text{B}(\mu\text{-OH})\text{B}(\text{OH})_3]^-$ will contribute to the ΔV^\ddagger value only slightly. It is also reasonable to consider that the forward reaction of eq 16 involves negative activation entropy, because a dimer formation decreases the number of free species.

Comparison with Related Reactions. One of us studied the mechanism of chelate formation between boric acid and 4-isopropyltropolone and chromotropic acid;¹² the kinetic parameters are compared in Table 1. The present exchange is much faster than the chelate formation, but the activation volumes are rather similar to one another. The reason is considered as follows.

We discussed that the rate-determining step of the chelate formation involves the association of boric acid with organic alcohol, i.e. first $\text{B}(\text{OH})\text{---C}$ bond formation between B(OH)_3 and the $\text{C}(\text{OH})$ group on the tropone or the naphthalene ring. The chelate-forming step which follows was reckoned to be fast. We now consider that the rate-determining step of the present exchange is the formation of the $\text{B}(\text{OH})\text{---B}$ bond, so that similar elementary processes are encountered at the rate-determining steps of the two types of reaction (Figure 8). The difference in single covalent radius between carbon and boron atom is ca. 0.1 \AA . The difference in volume of the spheres (radii $< 2 \text{ \AA}$) with a difference in radii of 0.1 \AA amounts to only ca. $2 \text{ cm}^3 \text{ mol}^{-1}$. This must be the reason why the observed ΔV^\ddagger values of Table 1 are similar to one another, and is consistent with our interpretation of the present reaction mechanism, although there can be different minor contributions to the observed ΔV^\ddagger values.

The remarkable difference in the rate of these two types of reaction is attributed to the large absolute value of negative activation entropy of the chelate formation (the difference of ΔH^\ddagger values cannot be discussed in detail because different kinds of atoms participate in the rate-determining step). We observed a significant deuterium effect on the rate of chelate formation and pointed out the importance of the hydrogen bond between boric acid and the organic moiety at the rate-determining step.¹² The rigid structure of the diol moiety of 4-isopropyltropolone and chromotropic acid must be responsible for the large negative activation entropy. Their OH groups on the aromatic ring can form hydrogen bonds with B(OH)_3 only when a favorable orientation is achieved. On the other hand, the steric requirement for the formation of $[(\text{HO})_3\text{B}(\mu\text{-OH})\text{B}(\text{OH})_3]^-$ should be far less restricted to give a negative activation entropy with relatively small absolute value.

(24) Tetrahedral B(OH)_4^- is naturally simulated by a sphere. Planar triangular B(OH)_3 is also likened to a sphere for the following reasons. The thermochemical ionic radii of the planar triangular oxoanions CO_3^{2-} and NO_3^- calculated by use of Kaputinskii's equation (1.85 and 1.89 \AA , respectively) are equal to their free rotation radii (Kaputinskii, A. F. *Q. Rev., Chem. Soc.* 1956, 10, 283). These ions are reckoned to have spherical electrostatic region in crystalline state. Hence there is a good reason to simulate the apparent shape of B(OH)_3 in solution to a sphere.

The isotopic exchange between various oxoanions XO_m^{n-} and solvent water molecule was extensively studied by ^{17}O NMR spectroscopy and ^{18}O labeling method.²⁵ Dissociative rate-determining steps involving the cleavage of X–O bond have been postulated for most kinds of oxoanions. Phosphoric acid seemed to be the unique exception in which a mechanism involving a dimer was suggested at high concentrations.²⁶ Boric acid has added another exception. These two oxoanions have a marked

overall trend to form stable polymers. Although the bridging structure of the polymerized form of phosphoric acid is different from our present intermediate, it is interesting to find that oxoanions with a great trend toward polymerization exchange oxygen through the dimeric form.

Acknowledgment. K.I. gratefully acknowledges financial support by grants from the Morino Foundation for Molecular Science and the Kawakami Memorial Foundation.

Supplementary Material Available: Observed chemical shifts, bandwidths, and rate constants at various temperatures and pressures (Tables SI–SV) (5 pages). Ordering information is given on any current masthead page.

-
- (25) Gamsjäger, H.; Murmann, R. K. In *Advances in Inorganic and Bioinorganic Chemistry*; Sykes, A. G., Ed.; Academic Press: London, 1983; Vol. 2, pp 317–380.
- (26) Keisch, B.; Kennedy, J. W.; Wahl, A. C. *J. Am. Chem. Soc.* **1958**, *80*, 4778.